THE JOURNAL OF PHYSICAL CHEMISTRY A

pubs.acs.org/JPCB

Article

Exchange-Correlation Energy Densities and Response Potentials: Connection between Two Definitions and Analytical Model for the Strong-Coupling Limit of a Stretched Bond

Published as part of The Journal of Physical Chemistry virtual special issue "Paul Geerlings Festschrift".

Sara Giarrusso* and Paola Gori-Giorgi*

Cite This: *J. Phys. Chem. A* 2020, 124, 2473−2482

Read Online

ACCESS | Metrics & More | Article Recommendations

ABSTRACT: We analyze in depth two widely used definitions (from the theory of conditional probability amplitudes and from the adiabatic connection formalism) of the exchange-correlation energy density and of the response potential of Kohn−Sham density functional theory. We introduce a local form of the coupling-constant-dependent Hohenberg−Kohn functional, showing that the difference between the two definitions is due to a corresponding local first-order term in the coupling constant, which disappears globally (when integrated over all space), but not locally. We also design an analytic representation for the response potential in the strong-coupling limit of density functional theory for a model single stretched bond.

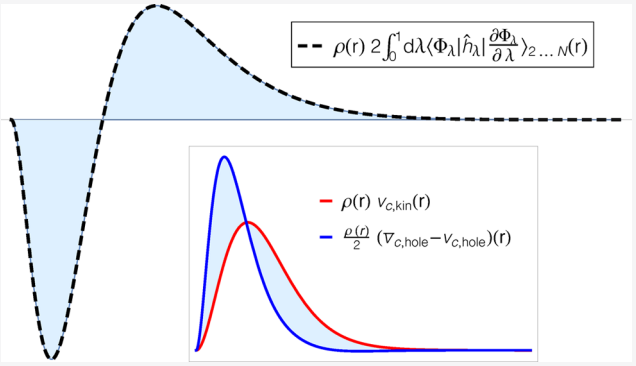

INTRODUCTION

In Kohn−Sham (KS) Density Functional Theory (DFT), the ground-state energy of a given chemical system is computed via an exact mapping onto a system of noninteracting electrons, the KS system, having the same one-electron density $n(\boldsymbol{r})$. The particles in the KS system feel the one-body KS potential, which forces them to have the prescribed density $n(\boldsymbol{r})$. The KS potential is built from parts that are exactly known (the external potential due to the nuclei and the Hartree potential, which gives a mean-field approximation for the effects of the electron−electron interaction), plus a part that needs to be approximated, the so-called exchange-correlation (XC) potential $v_{xc}(\boldsymbol{r})$, given by the functional derivative with respect to $n(\boldsymbol{r})$ of the unknown XC energy $E_{xc}[n]$.

Exact properties[1−20] of the XC potential have played, and continue to play, a central role in building new approximations. In particular, it has become clear over the years that LDA and GGA approximations miss certain nonintuitive features of the XC potential, such as "peaks" and "steps", which are crucial to predict static electric polarizabilities and band gaps, and to describe bond breaking and strongly correlated systems.[1,2,4,6−20]

Using the theory of conditional probability amplitudes,[21,22] Levy, Perdew, and Sahni[23] have introduced in the DFT context a Schrödinger-type equation for $\sqrt{n(\boldsymbol{r})}$, which was later used by Baerends and co-workers[2,4,6−8,24] to derive an insightful and exact decomposition of the XC potential into so-called kinetic, response, and XC-hole terms. They also showed that LDA and GGA approximations typically reproduce quite well only the XC hole part of the XC potential, and that features such as "peaks" and "steps" are due, respectively, to the kinetic and response parts. A slightly different, but related, decomposition of the XC potential arises when we write $E_{xc}[n]$ in terms of an integration along the adiabatic connection at fixed density:[25−27] in this case we have a coupling-constant averaged (CCA) XC-hole potential and a CCA response part,[28] due to the functional derivative of the pair-correlation function with respect to the density. Also in this case, LDA and GGA approximate functionals capture rather well the CCA XC-hole part, while missing completely the features of the response part.[28]

The purpose of this work is 2-fold: on the one hand, we further investigate the relationship between the two different decompositions, using a local form of the Hohenberg−Kohn functional along the adiabatic connection. On the other hand, we construct a simple analytic representation for the response potential in the strong-coupling limit of DFT for the case of a model stretched heteronuclear bond.

Received: November 11, 2019
Revised: March 1, 2020
Published: March 2, 2020

https://dx.doi.org/10.1021/acs.jpca.9b10538
J. Phys. Chem. A 2020, 124, 2473−2482

DECOMPOSITIONS OF THE XC POTENTIAL

We start by reviewing the two different definitions of response potential. The first one arises by using the theory of conditional probability amplitudes first developed by Hunter.[21,22] Following the work in refs 2 and 23, we partition the Hamiltonian for N electrons bound by the external (nuclear) potential $v(\boldsymbol{r})$ in three parts: the Hamiltonian for $N-1$ electrons (with $i = 2, \cdots, N$), the one-body terms acting on electron 1, and the remaining interaction between electron 1 (taken as the reference) and all the others

$$\hat{H}^N(\boldsymbol{r}, \boldsymbol{r}_2, \cdots, \boldsymbol{r}_N) = \hat{H}^{N-1}(\boldsymbol{r}_2, \cdots, \boldsymbol{r}_N) - \frac{\nabla_{\boldsymbol{r}}^2}{2} + v(\boldsymbol{r}) + \sum_{i=2}^{N} \frac{1}{|\boldsymbol{r} - \boldsymbol{r}_i|} \tag{1}$$

In the same spirit, we factorize the N-particle wave function

$$\Psi^N(\boldsymbol{r}\sigma, \mathbf{x}_2, \cdots, \mathbf{x}_N) = \sqrt{\frac{n(\boldsymbol{r})}{N}}\,\Phi(\sigma, \mathbf{x}_2, \cdots, \mathbf{x}_N; \boldsymbol{r}) \tag{2}$$

into the so-called *marginal* and *conditional (probability) amplitudes*, represented respectively by the square root of the density as a function of coordinates of electron 1 divided by the number of electrons N and a function of the other $N-1$ electronic positions, $\Phi(\sigma,\mathbf{x}_2,\cdots,\mathbf{x}_N;\boldsymbol{r})$, which depends on electron 1 in a parametric way. We consider here the case that the wave function Ψ is real. Physically speaking, $\Phi(\sigma,\mathbf{x}_2,\cdots,\mathbf{x}_N;\boldsymbol{r})$ is a sort of $(N-1)$-particle wave function that describes how the electronic cloud of $N-1$ electrons readjusts as a function of the position of electron 1. Indeed, its modulus square integrates to one for any value of the position vector of the reference electron

$$\int |\Phi(\sigma, \mathbf{x}_2, \cdots, \mathbf{x}_N; \boldsymbol{r})|^2 \, \mathrm{d}\sigma \, \mathrm{d}\mathbf{x}_2 \cdots \mathrm{d}\mathbf{x}_N = 1 \quad \forall\, \boldsymbol{r} \tag{3}$$

By applying eq 1 to eq 2, and by multiplying to the left both members by $\Phi^*(\sigma,\mathbf{x}_2,\cdots,\mathbf{x}_N;\boldsymbol{r})$ and integrating over the spin variable of the reference electron and on the spatial and spin variables of electrons 2,$\cdots$, N, we obtain a Schrödinger-like equation for $\sqrt{n(\boldsymbol{r})}$,

$$-\frac{\nabla^2}{2}\sqrt{n(\boldsymbol{r})} + v_{\mathrm{eff}}(\boldsymbol{r})\sqrt{n(\boldsymbol{r})} = -I\sqrt{n(\boldsymbol{r})} \tag{4}$$

where $I = E_0^{N-1} - E_0^N$ is the ionization potential. The resulting effective potential $v_{\mathrm{eff}}(\boldsymbol{r})$ is equal to

$$v_{\mathrm{eff}}(\boldsymbol{r}) = v(\boldsymbol{r}) + v_{\mathrm{cond}}(\boldsymbol{r}) + v_{\mathrm{kin}}(\boldsymbol{r}) + v_{N-1}(\boldsymbol{r}) \tag{5}$$

with

$$v_{\mathrm{cond}}(\boldsymbol{r}) = \int \frac{P_2(\boldsymbol{r}, \boldsymbol{r}')}{|\boldsymbol{r} - \boldsymbol{r}'|} \mathrm{d}\boldsymbol{r}\, \mathrm{d}\boldsymbol{r}' \tag{6}$$

where the subscript "cond" stands obviously for conditional and we have used the definition of the pair density, $P_2(\boldsymbol{r},\boldsymbol{r}')$,

$$P_2(\boldsymbol{r}, \boldsymbol{r}') = N(N-1) \int |\Psi(\boldsymbol{r}\sigma, \boldsymbol{r}'\sigma', \cdots, \boldsymbol{x}_N)|^2 \, \mathrm{d}\sigma \, \mathrm{d}\sigma' \, \mathrm{d}\boldsymbol{x}_3 \cdots \mathrm{d}\boldsymbol{x}_N \tag{7}$$

This potential is usually split into $v_{\mathrm{cond}}(\boldsymbol{r}) = v_{\mathrm{H}}(\boldsymbol{r}) + v_{\mathrm{xc,hole}}(\boldsymbol{r})$, where $v_{\mathrm{H}}(\boldsymbol{r})$ is the Hartree potential. We also define the exchange-correlation pair-distribution function, $g_{\mathrm{xc}}(\boldsymbol{r},\boldsymbol{r}')$,

$$g_{\mathrm{xc}}(\boldsymbol{r}, \boldsymbol{r}') = \frac{P_2(\boldsymbol{r}, \boldsymbol{r}')}{n(\boldsymbol{r})n(\boldsymbol{r}')} - 1 \tag{8}$$

and write $v_{\mathrm{xc,hole}}(\mathbf{r})$ as

$$v_{\mathrm{xc,hole}}(\mathbf{r}) = \int n(\mathbf{r}') \frac{g_{\mathrm{xc}}(\mathbf{r}, \mathbf{r}')}{|\mathbf{r} - \mathbf{r}'|} \, \mathrm{d}\mathbf{r}' \tag{9}$$

The term that comes from the kinetic energy operator acting on the conditional amplitude can be written, when we take into account eq 3, as

$$v_{\mathrm{kin}}(\boldsymbol{r}) = \frac{1}{2} \int |\nabla_{\boldsymbol{r}} \Phi(\sigma, \mathbf{x}_2, \cdots, \mathbf{x}_N; \boldsymbol{r})|^2 \, \mathrm{d}\sigma \, \mathrm{d}\mathbf{x}_2 \cdots \mathrm{d}\mathbf{x}_N \tag{10}$$

and it is called kinetic potential. Finally, the term coming from the $N-1$ Hamiltonian is equal to

$$v_{N-1}(\boldsymbol{r}) = \int \Phi^*(\sigma, \mathbf{x}_2, \cdots, \mathbf{x}_N; \boldsymbol{r}) \hat{H}^{N-1}(\boldsymbol{r}_2, \cdots, \boldsymbol{r}_N) \Phi(\sigma, \mathbf{x}_2, \cdots, \mathbf{x}_N; \boldsymbol{r}) \, \mathrm{d}\sigma \, \mathrm{d}\mathbf{x}_2 \cdots \mathrm{d}\mathbf{x}_N - E_0^{N-1} \tag{11}$$

where the shift E_0^{N-1} makes this potential vanish when $|\boldsymbol{r}| \to \infty$ (with the possible exception in certain directions, if there are nodal planes that extend to infinity[29−31]). It is evident that these three potentials are always positive, as in eqs 6 and 10 the integrands are squared quantities, and the right-hand-side of eq 11 must be positive by virtue of the variational principle.

Baerends and co-workers[2,4,6−8,24] have then repeated the same procedure for the KS Hamiltonian $\hat{H}_s^N$ with KS potential $v_s(\boldsymbol{r})$,

$$\hat{H}_s^N = -\sum_i^N \frac{\nabla_{\boldsymbol{r}_i}^2}{2} + \sum_{i=1}^N v_s(\boldsymbol{r}_i) \tag{12}$$

which has the same one-electron density of the physical interacting system, obtaining

$$v_{s,\mathrm{kin}}(\boldsymbol{r}) = \frac{1}{2} \sum_{i=1}^{H} \left| \nabla \frac{\psi_i(\boldsymbol{r})}{\sqrt{n(\boldsymbol{r})}} \right|^2 = \frac{1}{2n(\boldsymbol{r})} \sum_{i=1}^{H} |\nabla \psi_i(\boldsymbol{r})|^2 - \frac{|\nabla n(\boldsymbol{r})|^2}{8n(\boldsymbol{r})^2} \tag{13}$$

where $\psi_i(\boldsymbol{r})$ are the H occupied KS orbitals, and

$$v_{s,N-1}(\boldsymbol{r}) = \sum_{i=1}^{H} (\epsilon_H - \epsilon_i) \frac{|\psi_i(\boldsymbol{r})|^2}{n(\boldsymbol{r})} \tag{14}$$

where ϵ_H is the energy of the KS highest occupied molecular orbital (HOMO). The effective KS potential for the square root of the density is nothing but the sum of the foreshown potentials plus the KS potential itself (the conditional potential being absent as there is no Coulomb repulsion between the particles),

$$v_{\mathrm{eff}}(\boldsymbol{r}) = v_s(\boldsymbol{r}) + v_{s,\mathrm{kin}}(\boldsymbol{r}) + v_{s,N-1}(\boldsymbol{r}) \tag{15}$$

Since the one-electron density is the same for the physical and the KS system, then the right-hand sides of eqs 5 and 15 are also the same, providing an expression for v_{xc}

$$v_{\mathrm{xc}}(\boldsymbol{r}) = v_{c,\mathrm{kin}}(\boldsymbol{r}) + v_{\mathrm{resp}}(\boldsymbol{r}) + v_{\text{xc-hole}}(\boldsymbol{r}) \tag{16}$$

with the correlation kinetic potential $v_{c,\mathrm{kin}}(\boldsymbol{r})$ given by

$$v_{c,\mathrm{kin}}(\boldsymbol{r}) = v_{\mathrm{kin}}(\boldsymbol{r}) - v_{s,\mathrm{kin}}(\boldsymbol{r}) \tag{17}$$

and the response potential $v_{\mathrm{resp}}(\boldsymbol{r})$ equal to

$$v_{\mathrm{resp}}(\boldsymbol{r}) = v_{N-1}(\boldsymbol{r}) - v_{s,N-1}(\boldsymbol{r}) \tag{18}$$

https://dx.doi.org/10.1021/acs.jpca.9b10538
J. Phys. Chem. A 2020, 124, 2473−2482

Response Potential with Kinetic and Interaction Components. The reason why eq 18 is called the response potential is that from the definition of the XC energy,

$$E_{xc}[n] = \underbrace{\langle\Psi|\hat{T}|\Psi\rangle - T_s[n]}_{T_c[n]} + \underbrace{\langle\Psi|\hat{V}_{ee}|\Psi\rangle - U[\rho]}_{W_1[n]} \tag{19}$$

where Ψ is the exact many-body wave function of the system under study, $T_s[n]$ is the KS kinetic energy, and $U[n]$ is the Hartree energy, we also have the exact equation

$$E_{xc}[n] = \int n(\boldsymbol{r}) v_{c,\mathrm{kin}}(\boldsymbol{r})\, \mathrm{d}\boldsymbol{r} + \frac{1}{2}\int n(\boldsymbol{r}) v_{\text{xc-hole}}(\boldsymbol{r})\, \mathrm{d}\boldsymbol{r} \tag{20}$$

By taking the functional derivative with respect to the density of both sides of 20 we obtain

$$\begin{aligned} v_{xc}(\boldsymbol{r}) &= \frac{\delta E_{xc}[n]}{\delta n(\boldsymbol{r})} \\ &= v_{c,\mathrm{kin}}(\boldsymbol{r}) + v_{\mathrm{xc,hole}}(\boldsymbol{r}) + v^{\mathrm{resp}}_{c,\mathrm{kin}}(\boldsymbol{r}) + v^{\mathrm{resp}}_{\mathrm{xc,hole}}(\boldsymbol{r}) \end{aligned} \tag{21}$$

with

$$v^{\mathrm{resp}}_{c,\mathrm{kin}}(\boldsymbol{r}) = \int n(\boldsymbol{r}') \frac{\delta v_{c,\mathrm{kin}}(\boldsymbol{r}')}{\delta n(\boldsymbol{r})}\, \mathrm{d}\boldsymbol{r}' \tag{22}$$

and

$$v^{\mathrm{resp}}_{\mathrm{xc,hole}}(\boldsymbol{r}) = \frac{1}{2}\int \frac{n(\boldsymbol{r}')n(\boldsymbol{r}'')}{|\boldsymbol{r}' - \boldsymbol{r}''|} \frac{\delta g_{xc}(\boldsymbol{r}', \boldsymbol{r}'')}{\delta n(\boldsymbol{r})}\, \mathrm{d}\boldsymbol{r}'\, \mathrm{d}\boldsymbol{r}'' \tag{23}$$

By comparing eqs 16 and 21 we see that

$$v_{\mathrm{resp}}(\boldsymbol{r}) = v^{\mathrm{resp}}_{c,\mathrm{kin}}(\boldsymbol{r}) + v^{\mathrm{resp}}_{\mathrm{xc,hole}}(\boldsymbol{r}) \tag{24}$$

It has been shown that "peaks" in the KS potential come from $v_{c,\mathrm{kin}}(\boldsymbol{r})$,[2,10,17,32,33] while "steps" come from $v_{\mathrm{resp}}(\boldsymbol{r})$.[8,9,15,34] Also, notice that $v_{\mathrm{xc,hole}}(|\boldsymbol{r}| \to \infty) \sim -\frac{1}{|\boldsymbol{r}|}$, implying that all the other terms are shorter ranged.

Response Potential from the Coupling-Constant Integration. Another exact equation for $E_{xc}[n]$ can be obtained by considering the λ-dependent Hohenberg−Kohn (HK) functional in the Levy constrained-search formulation,[35] where the interaction is scaled by a real and positive coupling parameter λ, namely

$$F_\lambda[n] = \min_{\Psi\to n}\langle\Psi|\hat{T} + \lambda\hat{V}_{ee}|\Psi\rangle \tag{25}$$

where $F_1[n]$ is the universal HK functional of the physical system and $F_0[n]$ is equal to the KS kinetic energy $T_s[n]$. By simply plugging the wave function $\Psi_\lambda[n]$ that minimizes eq 25 in eqs 7 and 8, we define the pair-density $P_2^\lambda(\boldsymbol{r},\boldsymbol{r}')$ and the corresponding $g_{xc}^\lambda(\boldsymbol{r},\boldsymbol{r}')$. The CCA pair-correlation function $\overline{g}_{xc}(\boldsymbol{r},\boldsymbol{r}')$ is then defined as

$$\overline{g}_{xc}(\boldsymbol{r}, \boldsymbol{r}') = \int_0^1 g_{xc}^\lambda(\boldsymbol{r}, \boldsymbol{r}')\, \mathrm{d}\lambda \tag{26}$$

The XC energy can be written in terms of the CCA $\overline{g}_{xc}(\boldsymbol{r},\boldsymbol{r}')$,

$$E_{xc}[n] = \frac{1}{2}\iint n(\boldsymbol{r})n(\boldsymbol{r}')\frac{\overline{g}_{xc}(\boldsymbol{r}, \boldsymbol{r}')}{|\boldsymbol{r} - \boldsymbol{r}'|}\, \mathrm{d}\boldsymbol{r}\, \mathrm{d}\boldsymbol{r}' \tag{27}$$

as the integration over λ allows recovering the kinetic contribution to $E_{xc}[n]$.[25−27] Taking the functional derivative of eq 27 we obtain two terms[28]

$$v_{xc}(\boldsymbol{r}) = \frac{\delta E_{xc}[n]}{\delta n(\boldsymbol{r})} = \overline{v}_{\mathrm{xc,hole}}(\boldsymbol{r}) + \overline{v}_{\mathrm{resp}}(\boldsymbol{r}) \tag{28}$$

where

$$\overline{v}_{\mathrm{xc,hole}}(\boldsymbol{r}) = \int n(\boldsymbol{r}')\frac{\overline{g}_{xc}(\boldsymbol{r}, \boldsymbol{r}')}{|\boldsymbol{r} - \boldsymbol{r}'|}\, \mathrm{d}\boldsymbol{r}' \tag{29}$$

and

$$\overline{v}_{\mathrm{resp}}(\boldsymbol{r}) = \frac{1}{2}\iint \frac{n(\boldsymbol{r}')n(\boldsymbol{r}'')}{|\boldsymbol{r}' - \boldsymbol{r}''|}\frac{\delta \overline{g}_{xc}(\boldsymbol{r}', \boldsymbol{r}'')}{\delta n(\boldsymbol{r})}\, \mathrm{d}\boldsymbol{r}'\, \mathrm{d}\boldsymbol{r}'' \tag{30}$$

Again, also in this case $\overline{v}_{\mathrm{xc,hole}}(\boldsymbol{r})$ has the full asymptotic behavior $-\frac{1}{|\boldsymbol{r}|}$ at large $|\boldsymbol{r}|$ and the response part $\overline{v}_{\mathrm{resp}}(\boldsymbol{r})$ is shorter ranged. A decomposition in which the response part also contains $\frac{1}{2}\overline{v}_{\mathrm{xc,hole}}(\mathrm{r})$, has been proposed in ref 36. Comparing eqs 21 and 28, we have

$$\begin{aligned} &\overline{v}_{\mathrm{xc,hole}}(\boldsymbol{r}) + \overline{v}_{\mathrm{resp}}(\boldsymbol{r}) \\ &\quad = v_{c,\mathrm{kin}}(\boldsymbol{r}) + v_{\mathrm{xc,hole}}(\boldsymbol{r}) + v^{\mathrm{resp}}_{c,\mathrm{kin}}(\boldsymbol{r}) + v^{\mathrm{resp}}_{\mathrm{xc,hole}}(\boldsymbol{r}) \end{aligned} \tag{31}$$

One would naively expect that the response part in the left-hand side equals the sum of the response parts in the right-hand sides. However, this is not true, and in general we have

$$v^{\mathrm{resp}}_{c,\mathrm{kin}}(\boldsymbol{r}) + v^{\mathrm{resp}}_{\mathrm{xc,hole}}(\boldsymbol{r}) \neq \overline{v}_{\mathrm{resp}}(\boldsymbol{r}) \tag{32}$$

$$v_{c,\mathrm{kin}}(\boldsymbol{r}) + v_{\mathrm{xc,hole}}(\boldsymbol{r}) \neq \overline{v}_{\mathrm{xc,hole}}(\boldsymbol{r}) \tag{33}$$

It is one of the purposes of this work to further investigate and analyze the difference between these two response potentials. Notice that, if we split the potential into its exchange (X) and correlation (C) components, for the X part the two definitions become equivalent, as there is no kinetic and no λ dependence in exchange, $\overline{v}_{x,\mathrm{hole}} = v_{x,\mathrm{hole}}$.

ANALYSIS OF ENERGY DENSITIES AND RESPONSE POTENTIALS WITHIN THE TWO DEFINITIONS

The two ways to write the XC energy reviewed in the previous section, from the conditional amplitude formalism and from the adiabatic connection, stem from the two different energy densities (sometimes called gauges)

$$\epsilon_{\mathrm{kin+hole}}(\boldsymbol{r}) = v_{c,\mathrm{kin}}(\boldsymbol{r}) + \frac{1}{2}v_{\mathrm{xc,hole}}(\boldsymbol{r}) \tag{34}$$

$$\epsilon_{xc}(\boldsymbol{r}) = \frac{1}{2}\overline{v}_{\mathrm{xc,hole}}(\boldsymbol{r}) \tag{35}$$

which both yield the same $E_{xc}[n]$ when multiplied by the density and integrated over all space. The second definition, $\epsilon_{xc}(\boldsymbol{r})$, is the one most commonly used in DFT, also called the XC-hole potential gauge. By rewriting it as

$$\epsilon_{xc}(\boldsymbol{r}) = \frac{1}{2}v_{\mathrm{xc,hole}}(\boldsymbol{r}) + \left(\frac{1}{2}\overline{v}_{c,\mathrm{hole}}(\boldsymbol{r}) - \frac{1}{2}v_{c,\mathrm{hole}}(\boldsymbol{r})\right) \tag{36}$$

we see that the difference between the two definitions stem from how they describe the correlation kinetic energy density, as both $v_{c,\mathrm{kin}}(\boldsymbol{r})$ and $\frac{1}{2}\overline{v}_{c,\mathrm{hole}}(\boldsymbol{r}) - \frac{1}{2}v_{c,\mathrm{hole}}(\boldsymbol{r})$ integrate to $T_c[n]$ when multiplied by $n(\boldsymbol{r})$. These two kinetic energy densities are in general rather different, as shown, for example, in Figure 1 for the H^- anion, or in Figure 14 of ref 37 for the Hooke's atom series. An exception is the uniform electron gas case (including

https://dx.doi.org/10.1021/acs.jpca.9b10538
J. Phys. Chem. A 2020, 124, 2473−2482

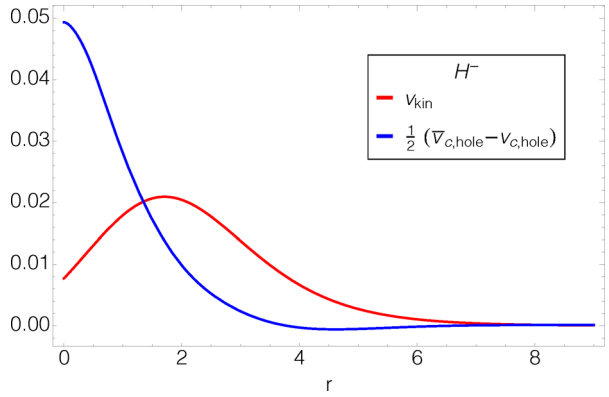

Figure 1. Two possible kinetic correlation energy densities, from the conditional amplitude formalism and from the coupling-constant average of the interaction part. Notice that in this case, as $N = 2$ we have $v_{c,\mathrm{kin}} = v_{\mathrm{kin}}$. The potential v_{kin} has been computed from the accurate wave function of ref 40, while $\bar{v}_{c,\mathrm{hole}}$ and $v_{c,\mathrm{hole}}(\boldsymbol{r})$ are obtained from refs 41−46.

the finite ones[38,39]), in which the kinetic energy density is a constant and thus the same in both definitions. The local-density approximation (LDA) can then be interpreted, in each point of space, as an approximation for either of the two gauges. The gauge of semilocal functional is a more subtle issue, as many of them rely on integration by parts.

Both energy density definitions of eqs 34 and 35 go like $-\frac{1}{2|\boldsymbol{r}|}$ at large $|\boldsymbol{r}|$. The total functional derivative is obviously the same, as in eq 31), and has the well-known large-$|\boldsymbol{r}|$ behavior $-\frac{1}{|\boldsymbol{r}|}$, thus two times the one of the energy density. Semilocal approximate functionals typically miss both asymptotic behaviors. It is possible to fix the energy density long-range behavior in a semilocal functional for a specific density decay (e.g., ref 47 for exponentially decaying density), but then the factor 2 in the functional derivative will be missing. It is also possible to fix, instead, the behavior of the XC potential, but in this case the asymptotics of the energy density will be spoiled.[36,48] Functionals such as the exact exchange case or range-separated hybrids do not suffer from this issue although these latters are often used in the generalized KS formalism[49] giving away the multiplicative character of the potential. The strictly correlated electrons (SCE) functional, corresponding to the $\lambda \to \infty$ limit of the adiabatic connection, is one of the very few currently available functionals that are able to capture both asymptotic behaviors[50] in a pure KS framework. However, existing approximations inspired to the SCE mathematical structure, which use integrals of the density as basic ingredient,[51−53] are, again, only able to capture the exact energy density asymptotics but not the one of the XC potential, missing the factor 2.

Here we want to further analyze the difference between the two possible definitions of the energy densities and of the response part of the XC potential. Let us first introduce the new quantity $f_\lambda[n](\boldsymbol{r})$

$$f_\lambda[n](\boldsymbol{r}) = \int \Phi_\lambda^*(\sigma, \boldsymbol{x}_2, \cdots, \boldsymbol{x}_N; \boldsymbol{r})\left(-\frac{\nabla_r^2}{2} + \frac{\sum_{i=2}^N}{2}\frac{\lambda}{r_{1i}}\right) \Phi_\lambda(\sigma, \boldsymbol{x}_2, \cdots, \boldsymbol{x}_N; \boldsymbol{r})\, \mathrm{d}\sigma\, \mathrm{d}\boldsymbol{r}_2 \cdots \boldsymbol{r}_N \tag{37}$$

which defines something close to an energy density for the λ-dependent HK functional in the Levy constrained formulation of eq 25, in the sense that it holds

$$\int n(\boldsymbol{r}) f_\lambda[n](\boldsymbol{r})\, \mathrm{d}\boldsymbol{r} = F_\lambda[n] - T_{\mathrm{W}}[n] \tag{38}$$

where T_{W} is the Von Weizsäcker kinetic energy functional, clearly independent of λ. The conditional amplitude Φ_λ is obtained by plugging the wave function Ψ_λ that minimizes eq 25 into eq 2. However, Φ_λ will not be in general the minimizer of $\hat{h}_\lambda = -\frac{\nabla_r^2}{2} + \frac{\sum_{i=2}^N}{2}\frac{\lambda}{r_{1i}}$ at a given $\boldsymbol{r}$. By differentiating with respect to λ both sides of eq 37 we then obtain

$$\frac{\partial}{\partial\lambda} f_\lambda(\boldsymbol{r}) = \left(\langle \Phi_\lambda | \frac{\partial \hat{h}_\lambda}{\partial\lambda} | \Phi_\lambda \rangle_{2\ldots N} + \langle \frac{\partial \Phi_\lambda}{\partial\lambda} | \hat{h}_\lambda | \Phi_\lambda \rangle_{2\ldots N} + \langle \Phi_\lambda | \hat{h}_\lambda | \frac{\partial \Phi_\lambda}{\partial\lambda} \rangle_{2\ldots N} \right)(\boldsymbol{r}) \tag{39}$$

where the Dirac brakets $\langle \cdots | \cdots \rangle_{2\cdots N}$ stand for $\int \mathrm{d}\sigma\, \mathrm{d}\boldsymbol{x}_2 \cdots \boldsymbol{x}_N$. We set

$$\langle \frac{\partial \Phi_\lambda}{\partial\lambda} | \hat{h}_\lambda | \Phi_\lambda \rangle_{2\ldots N} + \langle \Phi_\lambda | \hat{h}_\lambda | \frac{\partial \Phi_\lambda}{\partial\lambda} \rangle_{2\ldots N} = 2 \langle \Phi_\lambda | \hat{h}_\lambda | \frac{\partial \Phi_\lambda}{\partial\lambda} \rangle_{2\ldots N}$$

as we assumed Φ_λ to be real. We then simply write

$$f_1(\boldsymbol{r}) - f_0(\boldsymbol{r}) = \int_0^1 \mathrm{d}\lambda \left(\frac{\partial}{\partial\lambda} f_\lambda(\boldsymbol{r}) \right) \tag{40}$$

Evaluating the left-hand side, we immediately get

$$f_1(\boldsymbol{r}) - f_0(\boldsymbol{r}) = v_{c,\mathrm{kin}}(\boldsymbol{r}) + \frac{1}{2} v_{\mathrm{cond}}(\boldsymbol{r}) \tag{41}$$

But we also have

$$\langle \Phi_\lambda | \frac{\partial \hat{h}_\lambda}{\partial\lambda} | \Phi_\lambda \rangle_{2\ldots N}(\boldsymbol{r}) = \frac{1}{2} \int \frac{n(\boldsymbol{r}')(g_{\mathrm{xc}}^\lambda(\boldsymbol{r}, \boldsymbol{r}') + 1)}{|\boldsymbol{r} - \boldsymbol{r}'|}\, \mathrm{d}\boldsymbol{r}' \tag{42}$$

so that combining eqs 39, 41, and 42 and subtracting the Hartree potential from both sides we find the relation

$$\frac{1}{2}\bar{v}_{xc\text{-hole}} = v_{c,\mathrm{kin}} + \frac{1}{2} v_{\mathrm{xc\text{-}hole}} - 2\int_0^1 \mathrm{d}\lambda \langle \Phi_\lambda | \hat{h}_\lambda | \frac{\partial \Phi_\lambda}{\partial\lambda} \rangle_{2\ldots N} \tag{43}$$

We then see that the difference between the two energy densities of eqs 34 and 35 is given by the term

$$\epsilon_{\mathrm{kin+hole}} - \epsilon_{\mathrm{xc}} = 2\int_0^1 \mathrm{d}\lambda \langle \Phi_\lambda | \hat{h}_\lambda | \frac{\partial \Phi_\lambda}{\partial\lambda} \rangle_{2\ldots N} \tag{44}$$

When multiplied by the density and integrated over all space, the right-hand side of eq 44 integrates to zero by virtue of the Hellmann−Feynman theorem, as Ψ_λ is the minimizer of eq 25. The two energy densities are then different because the first-order term in λ does not disappear locally, but only globally. We see that they are also equal, as should be, for exchange-only, as in that case the conditional amplitude Φ does not depend on λ. By combining eqs 43 and 31, we can also find a relation between the two response potentials

$$\bar{v}_{\mathrm{resp}} = v_{\mathrm{resp}} - v_{c,\mathrm{kin}} + 4\int_0^1 \mathrm{d}\lambda \langle \Phi_\lambda | \hat{h}_\lambda | \frac{\partial \Phi_\lambda}{\partial\lambda} \rangle_{2\ldots N} \tag{45}$$

https://dx.doi.org/10.1021/acs.jpca.9b10538
J. Phys. Chem. A 2020, 124, 2473−2482

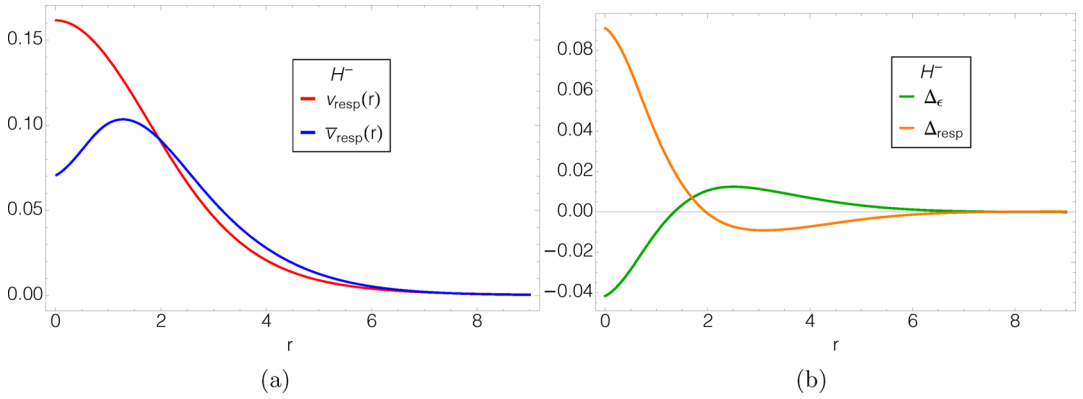

Figure 2. Comparison between v_{resp} and $\bar{v}_{resp}$ (left panel) and between Δ_ϵ and Δ_{resp} (right panel) for the hydrogen anion. The potential v_{resp} has been computed from the correlated wave functions of ref 40, while $\bar{v}_{resp}$ is obtained from refs 41−46.

Note that eqs 44 and 45 are completely general results: they hold for any number of electrons and rely only on the few assumptions mentioned, that is, that the Levy-Lieb λ-dependent functional is differentiable at any λ and that the wave function Ψ_λ is real.

To explore their meaning, we start from the known relations between the global quantities $V_{ee}^{\lambda}[n] = \langle \Psi_\lambda[n]|\hat{V}_{ee}|\Psi_\lambda[n]\rangle$ and $T^{\lambda}[n] = \langle \Psi_\lambda[n]|\hat{T}|\Psi_\lambda[n]\rangle$, that is,[54]

$$\frac{\partial}{\partial\lambda}V_{ee}^{\lambda}[n] \leq 0 \tag{46}$$

$$\frac{\partial}{\partial\lambda}T^{\lambda}[n] = -\lambda\frac{\partial}{\partial\lambda}V_{ee}^{\lambda}[n] \tag{47}$$

Defining

$$v_{\lambda,\mathrm{cond}}(\boldsymbol{r}) = \int\sum_{i=2}^{N}\frac{1}{|\boldsymbol{r}-\boldsymbol{r}_i|}|\Phi_\lambda(\sigma, \boldsymbol{x}_2, \cdots, \boldsymbol{x}_N; \boldsymbol{r})|^2\,\mathrm{d}\sigma\,\mathrm{d}\mathbf{x}_2 \cdots \mathrm{d}\mathbf{x}_N \tag{48}$$

in agreement with eq 6, and considering that

$$\frac{\partial}{\partial\lambda}V_{ee}^{\lambda}[n] = \frac{1}{2}\int n(\boldsymbol{r})\frac{\partial}{\partial\lambda}v_{\lambda,\mathrm{cond}}(\boldsymbol{r})[n]\,\mathrm{d}\boldsymbol{r} \tag{49}$$

the natural doppelganger of eq 46 at the local level would concern $\frac{\partial}{\partial\lambda}v_{\lambda,\mathrm{cond}}[n](\boldsymbol{r})$. However, precisely because Φ_λ is not stationary with respect to the expectation value of $\hat{h}_\lambda$,

$$\langle\Phi_\lambda|\hat{h}_\lambda|\Phi_\lambda\rangle(\boldsymbol{r}) \lessapprox \langle\Phi_{\lambda'}|\hat{h}_\lambda|\Phi_{\lambda'}\rangle(\boldsymbol{r}) \quad \forall\ \boldsymbol{r} \tag{50}$$

we cannot perform the usual steps (as in ref 54) and in general there will be regions in the domain of the density where

$$\frac{\partial}{\partial\lambda}v_{\lambda,\mathrm{cond}}[n](\boldsymbol{r}) \geq 0 \quad \text{for } \boldsymbol{r}' < \boldsymbol{r} < \boldsymbol{r}'' \tag{51}$$

Such regions have been observed for example, for the case of the Hooke's atom at pronounced correlation (very low frequency, ω, of the binding harmonic potential) in ref 50. They are expected to occur mostly where the density is negligeable (such as in the tail) as a combination of eqs 49 and 46 requires them to contribute to a lesser extent than those regions where $\frac{\partial}{\partial\lambda}v_{\lambda,\mathrm{cond}}[n](\boldsymbol{r}) \leq 0$. Lack of a "local variational principle", as expressed in eq 50, has further consequences: using that $\langle\Phi_\lambda|\hat{h}_\lambda|\frac{\partial\Phi_\lambda}{\partial\lambda}\rangle_{2\ldots N}$ does not vanish in general as already discussed and splitting this term into its contributions

$$\langle\Phi_\lambda|\hat{h}_\lambda|\frac{\partial\Phi_\lambda}{\partial\lambda}\rangle_{2\ldots N} = \frac{1}{2}\left(\frac{\partial}{\partial\lambda}v_{\lambda,\mathrm{kin}}(\boldsymbol{r}) + \frac{\lambda}{2}\frac{\partial}{\partial\lambda}v_{\lambda,\mathrm{cond}}(\boldsymbol{r})\right) \tag{52}$$

with

$$v_{\lambda,\mathrm{kin}}(\boldsymbol{r}) := \frac{1}{2}\int|\nabla_{\boldsymbol{r}}\Phi_\lambda(\sigma, \boldsymbol{x}_2, \cdots, \boldsymbol{x}_N; \boldsymbol{r})|^2\mathrm{d}\sigma\,\mathrm{d}\mathbf{x}_2 \cdots \mathrm{d}\mathbf{x}_N \tag{53}$$

leads to the conclusion that also the local doppelganger of eq 47 is not satisfied, that is,

$$\frac{\partial}{\partial\lambda}v_{\lambda,\mathrm{kin}}(\boldsymbol{r}) \neq -\frac{\lambda}{2}\frac{\partial}{\partial\lambda}v_{\lambda,\mathrm{cond}}(\boldsymbol{r}) \tag{54}$$

The sign of $\frac{\partial}{\partial\lambda}v_{\lambda,\mathrm{kin}}(\boldsymbol{r})$ will be positive at least in the regions where the density is significant, to satisfy eq 47 or, equivalently, $\int v_{c,\mathrm{kin}}(\boldsymbol{r})n(\boldsymbol{r})\mathrm{d}\boldsymbol{r} = T_c \geq 0$, but we cannot exclude that in some regions of lower density $\frac{\partial}{\partial\lambda}v_{\lambda,\mathrm{kin}}(\boldsymbol{r})$ could be negative. Nevertheless, we expect the terms $\frac{\partial}{\partial\lambda}v_{\lambda,\mathrm{kin}}(\boldsymbol{r})$ and $\frac{\lambda}{2}\frac{\partial}{\partial\lambda}v_{\lambda,\mathrm{cond}}(\boldsymbol{r})$, that are responsible of the difference between CCA and nonaveraged quantities (i.e., ϵ_{xc}, $\bar{v}_{resp}$ and $\epsilon_{kin+hole}$, v_{resp}) according to eqs 44 and 45, to work mainly in opposite directions. Combining eqs 36, 43, 44, and 45, we can rearrange the differences $\Delta_\epsilon := \epsilon_{kin+hole} - \epsilon_{xc}$ and $\Delta_{resp} := v_{resp} - \bar{v}_{resp}$ as follows

$$\Delta_\epsilon = v_{c,\mathrm{kin}} - \frac{1}{2}(\bar{v}_{c,\mathrm{hole}} - v_{c,\mathrm{hole}}) \tag{55}$$

$$\Delta_{resp} = (\bar{v}_{c,\mathrm{hole}} - v_{c,\mathrm{hole}}) - v_{c,\mathrm{kin}} \tag{56}$$

which clearly shows that Δ_ϵ and Δ_{resp}, although constrained by eq 31, do not trivially "compensate" each other, because of the factor $\frac{1}{2}$ in front of $(\bar{v}_{c,\mathrm{hole}} - v_{c,\mathrm{hole}})$ present in the former and not in the latter difference. It might well be, then, that in regions where $|\Delta_\epsilon|$ is relatively small $|\Delta_{resp}|$ is instead much larger. This different redistribution between coupling-constant averaged and non-averaged terms into which the XC potential can be decomposed is quite subtle and inherently absent from an LDA model as well as from the SCE reference state (see refs 46 and 55 and discussion in the next section). In Figure 2, examples of v_{resp} and $\bar{v}_{resp}$ (left panel) and a comparison between Δ_ϵ and Δ_{resp} (right panel) is given for the hydrogen anion. Inspection of Figure 2 shows that the two response potentials have maxima located at different positions[46] and that, whereby the two energy densities have relatively close values (compare also Figure 1),

https://dx.doi.org/10.1021/acs.jpca.9b10538
J. Phys. Chem. A 2020, 124, 2473−2482

the values taken by the two different response potentials are more far apart (e.g., while $|\Delta_c|(r = 1) \simeq 0.01$, $|\Delta_{resp}|(r = 1) \simeq 0.04$). For the He atom, the quantities Δ_c and Δ_{resp} differ even more, indeed we find $|\Delta_c|(r = 0.5) \simeq 0.002$ while $|\Delta_{resp}|(r = 0.5) \simeq 0.030$ (not reported in the figure). These showcases stress the point that design of an approximate energy density functional in either chosen gauge should come along with that of an approximate response potential consistent with that gauge.

Another paradigmatic case is the one of a two-electron system *dissociating* into two one-electron fragments, which is often used to test and understand the problems of approximate DFT in describing bond breaking.[2,9,10,16,18] In this case, we have $\hat{h}_\lambda \sim -\frac{\nabla_{r_2}^2}{2}$, and then

$$\int_0^1 d\lambda \langle \Phi_\lambda | \hat{h}_\lambda | \frac{\partial \Phi_\lambda}{\partial \lambda} \rangle_{2\dots N} \sim \frac{1}{2} v_{c,\mathrm{kin}} \tag{57}$$

which plugged into eqs 43 and 45 gives

$$v_{xc,\mathrm{hole}}(x) \sim \overline{v}_{xc,\mathrm{hole}}(x) \tag{58}$$

$$\overline{v}_{\mathrm{resp}}(x) \sim v_{c,\mathrm{kin}}(x) + v_{\mathrm{resp}}(x) \tag{59}$$

as we had already conjectured in eq 83 of ref 46. Understanding the different roles played by the correlation response potential according to how the kinetic correlation is encoded in the different gauges is important to be able to model it. For example, in the case studied in ref 46, it has been observed that while the two inflection points of the step structure of v_{resp} signal where the exponential decay of the total density switches from that of the less electronegative fragment to that of the more electronegative one and viceversa, $\overline{v}_{\mathrm{resp}}$ has its global maximum located at the distance for which each fragment integrates to an integer number of electrons, a feature which clarifies how the KS potential is able to dissociate a bond into physical fragments (with integer number of electrons).

ANALYTICAL 1D MODEL FOR V_{HXC}^{SCE} AND V_{RESP}^{SCE} IN THE DISSOCIATION LIMIT

We now consider the strictly correlated electron (SCE) XC functional, which is given by

$$W_{\mathrm{SCE}}[n] = \lim_{\lambda\to\infty} \lambda^{-1} F_\lambda[n] - U[\rho] \tag{60}$$

and provides an extreme approximation for the XC energy, which becomes asymptotically exact when the system is driven to low density.[56,57] We focus on a prototypical model, often used to understand, test and improve approximations in DFT,[9,10,16,18,46] consisting of a one-dimensional (1D) system of $N = 2$ electrons dissociating into two one-electron fragments, mimicking the breaking of a single bond. The response potential $v_{\mathrm{resp}}^{\mathrm{SCE}}$ for the SCE functional was analyzed in ref 46, where it was found that, although $v_{\mathrm{resp}}^{\mathrm{SCE}}$ does not saturate as the exact response potential, it behaves very differently from semilocal functionals, with qualitative features much closer to the exact ones. Here we go one step further with respect to ref 46 and build a simple analytic model for $v_{\mathrm{resp}}^{\mathrm{SCE}}$ which works extremely well. This could be of interest, for example, in transport calculations for model systems,[58] but also as a starting point for new approximations.

We thus consider the following model for a heteronuclear diatomic molecule

$$n(x) = n_a\left(x - \frac{R}{2}\right) + n_b\left(x + \frac{R}{2}\right) = \frac{a}{2} e^{-a|x-R/2|} + \frac{b}{2} e^{-b|x+R/2|} \tag{61}$$

where a and b mimic the different ionization potentials of the "atoms" (pseudopotentials or frozen cores) and the density is normalized to 2. We have chosen $a > b$, therefore the more electronegative atom will be found to the right side of the origin (at a distance $+\frac{R}{2}$ from it) and the less electronegative to the left. The SCE functional of eq 60 for a two-electron system is given by[59−61]

$$W_{\mathrm{SCE}}[n] = \frac{1}{2}\int \frac{n(\boldsymbol{r})}{|\boldsymbol{r} - \mathbf{f}(\boldsymbol{r}, [n])|} d\boldsymbol{r} - U[n] \tag{62}$$

where the comotion function $\mathbf{f}(\boldsymbol{r}, [n])$ determines the position of the second electron as a function of the position $\boldsymbol{r}$ of the first one and it is a nonlocal functional of the density. Despite this extreme nonlocality, its functional derivative

$$v_{H\mathrm{xc}}^{\mathrm{SCE}}(\boldsymbol{r}) = \frac{\delta W_{\mathrm{SCE}}[n]}{\delta n(\boldsymbol{r})} + v_{\mathrm{H}}(\boldsymbol{r}) \tag{63}$$

can be computed from the exact force equation[60,62]

$$\nabla v_{H\mathrm{xc}}^{\mathrm{SCE}}(\boldsymbol{r}) = -\frac{\boldsymbol{r} - \mathbf{f}(\boldsymbol{r})}{|\boldsymbol{r} - \mathbf{f}(\boldsymbol{r})|^3} \tag{64}$$

And for the response potential, we have[46]

$$v_{\mathrm{resp}}^{\mathrm{SCE}}(\mathbf{r}) = v_{H\mathrm{xc}}^{\mathrm{SCE}}(\boldsymbol{r}) - \frac{1}{|\boldsymbol{r} - \mathbf{f}(\boldsymbol{r})|} \tag{65}$$

Notice that in the SCE limit there is no difference between $\overline{v}_{\mathrm{resp}}$ and v_{resp}, as SCE has the same scaling of exchange[63] or, equivalently, there is no kinetic correlation component to leading order in the $\lambda \to \infty$ limit. By defining

$$a_R: \int_{-\infty}^{aR} n(x)\, dx = 1 \tag{66}$$

the exact 1D comotion function is given by[59,64]

$$f(x) = \begin{cases} N_e^{-1}[N_e(x) + 1] & x < a_R \\ N_e^{-1}[N_e(x) - 1] & x > a_R \end{cases} \tag{67}$$

In ref 46, it has been shown that the shape of the comotion function for the density of eq 61 becomes asymptotically the same at any internuclear distance ("saturation" phenomenon), behaving, in particular, as a constant in the asymptotic regions $x \ll 1$ and $x \gg 1$ and as a linear curve with coefficients, $m^< = \frac{b}{a}$ and $m^> = \frac{a}{b}$ close to a_R. If we now approximate the small regions where the comotion function switches from the constant to the linear behavior and those where it diverges (it is sufficient to know each one of such regions only for one branch, as the comotion is symmetric with respect to the axis $y = x$) with sharp angles, we can determine the asymptotic ($R \to \infty$) comotion function

https://dx.doi.org/10.1021/acs.jpca.9b10538
J. Phys. Chem. A 2020, 124, 2473−2482

$$f_{\mathrm{mod}}(y) = \begin{cases} a_R & y \le x_T^< \\ m^< y + c^< & x_T^< < y < a_R \\ \infty & y = a_R \\ m^> y + c^> & a_R < y \le x_T^> \\ a_R & y > x_T^> \end{cases} \tag{68}$$

where $x_T^<$ ($x_T^>$) is the distance at which the comotion function switches from constant (linear) to linear (constant), while $c^<$ ($c^>$) is the constant shifting of the zero of the linear region to the negative (positive) x-axis. Note that, in devising the structure of 68, we can regardless choose whether $f_{\mathrm{mod}}(a_R) = \infty$ or $f_{\mathrm{mod}}(a_R) = -\infty$. The same is true for the inequalities, where we have either $f_{\mathrm{mod}}(x_T^<) = a_R$ or $f_{\mathrm{mod}}(x_T^<) = m^< y + c^<$. Such single point choices do not affect the SCE Hartree XC potential, as it is obtained from an integral expression containing f_{mod}, or the SCE response potential, as long as $f_{\mathrm{mod}}(a_R)$ diverges.

Assuming that eq 68 is a good model for the comotion function, we need very few considerations to determine all the quantities needed to calculate the SCE potential and its response part from it. In particular, considering the two identical right

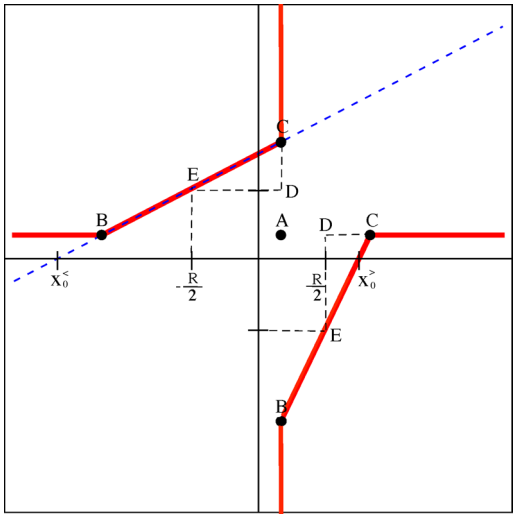

Figure 3. Asymptotic comotion function of eq 68.

triangles ABC plotted in Figure 3, where the point A is A = $\{a_R, a_R\}$, we can determine their catheti $\overline{\mathrm{AB}}$ and $\overline{\mathrm{AC}}$ from

$$\begin{cases} \overline{\mathrm{AB}}(\overline{\mathrm{AC}})^{-1} = \dfrac{a}{b} \\ \overline{\mathrm{AB}} + \overline{\mathrm{AC}} = 2R \end{cases} \tag{69}$$

where the first equation follows directly from eq 78 of ref 46, while the second is an extension of the discussion contained in section 5.2 of the same work, but it takes a bit more detail to support it. When the reference electron is situated slightly off $-\frac{R}{2}$, say $-\frac{R}{2} + \epsilon$ the second electron will be displaced by an amount $\frac{b}{a}\epsilon$ by the property of the right triangles.

Let us now consider the displacement from $-\frac{R}{2}$ to a_R, corresponding to the $\overline{\mathrm{DE}}$ segment in Figure 3. The comotion then increases by an amount $\frac{b}{a}\left(\frac{R}{2} + a_R\right)$ (the $\overline{\mathrm{DC}}$ segment in the figure). On the other hand, because of its symmetry, the displacement of the comotion on one branch corresponds to the displacement of the variable of the reference electron on the other branch. Furthermore, what happens from $-\frac{R}{2}$ *"onward"* must be mirrored by what happens from $-\frac{R}{2}$ *"backward"* bringing us to the conclusion that the segment

$$\overline{\mathrm{AB}} + \overline{\mathrm{AC}} = 2\left(\left(1 + \frac{b}{a}\right)\frac{R}{2} + \left(1 + \frac{b}{a}\right)a_R\right) = 2R$$

Once $\overline{\mathrm{AB}}$ and $\overline{\mathrm{AC}}$ are known, evaluating all the quantities specifying the asymptotic comotion in eq 68 is just a matter of basic trigonometry, providing

$$\begin{aligned} x_T^< &= -(\overline{\mathrm{AB}} - a_R) \\ x_T^> &= a_R + \overline{\mathrm{AC}} \\ x_0^< &= x_T^< - \frac{a}{b}a_R \\ x_0^> &= x_T^> - \frac{b}{a}a_R \\ c^< &= -m^< x_0^< \\ c^> &= -m^> x_0^> \end{aligned} \tag{70}$$

where $x_0^<$ ($x_0^>$) is the zero of the function $m^< x + c^<$ ($m^> x + c^>$), see Figure 3.

The modeled Hartree XC SCE potential, $v_{\mathrm{Hxc,mod}}^{\mathrm{SCE}}$, obtained from

$$v_{\mathrm{Hxc,mod}}^{\mathrm{SCE}}(x) = -\int_{-\infty}^{x} (f_{\mathrm{mod}}(y) - y)^{-2}\, \mathrm{d}y \tag{71}$$

(see eq 64), compares nicely with the numerically exact one as shown in the left column of Figure 4. In addition to the profile of the modeled potential, we report in Table 1, the values obtained for the maximum, which is the most delicate point.

The analytical expression for the dependence of the maximum of the Hartree XC SCE we obtain is

$$v_{\mathrm{Hxc}}^{\mathrm{SCE}}(a_R) = \frac{(a+b)^2}{2abR} \tag{72}$$

Equation 72 shows that when the two fragment densities are equal, the maximum value decreases like $\frac{2}{R}$, thus missing the exact behavior in which this value should saturate and become R-independent at large R. Note that when $a > b$, the maximum value decreases like $\frac{2}{R}\varsigma$, where ς is a factor greater than one. In this sense, the repulsion is at a minimum when the two densities are identical.

In the right column of Figure 4, we report the comparison between the modeled and the numerical SCE response potentials, obtained using the exact relation[46]

$$v_{\mathrm{resp}}^{\mathrm{SCE}}(x) = -v^{\mathrm{SCE}}(f(x)) + v^{\mathrm{SCE}}(a_R) \tag{73}$$

It is quite interesting to notice that the SCE response potential resulting from our model comotion eq 68 shows a pointwise jump in $x = a_R$. It is evident that, in order to correctly describe how this potential behaves around its maximum, we need to include also the knowledge of how the comotion function diverges, while this information is not needed in the case of the maximum of the SCE Hartree XC potential. Nonetheless, our

https://dx.doi.org/10.1021/acs.jpca.9b10538
J. Phys. Chem. A 2020, 124, 2473−2482

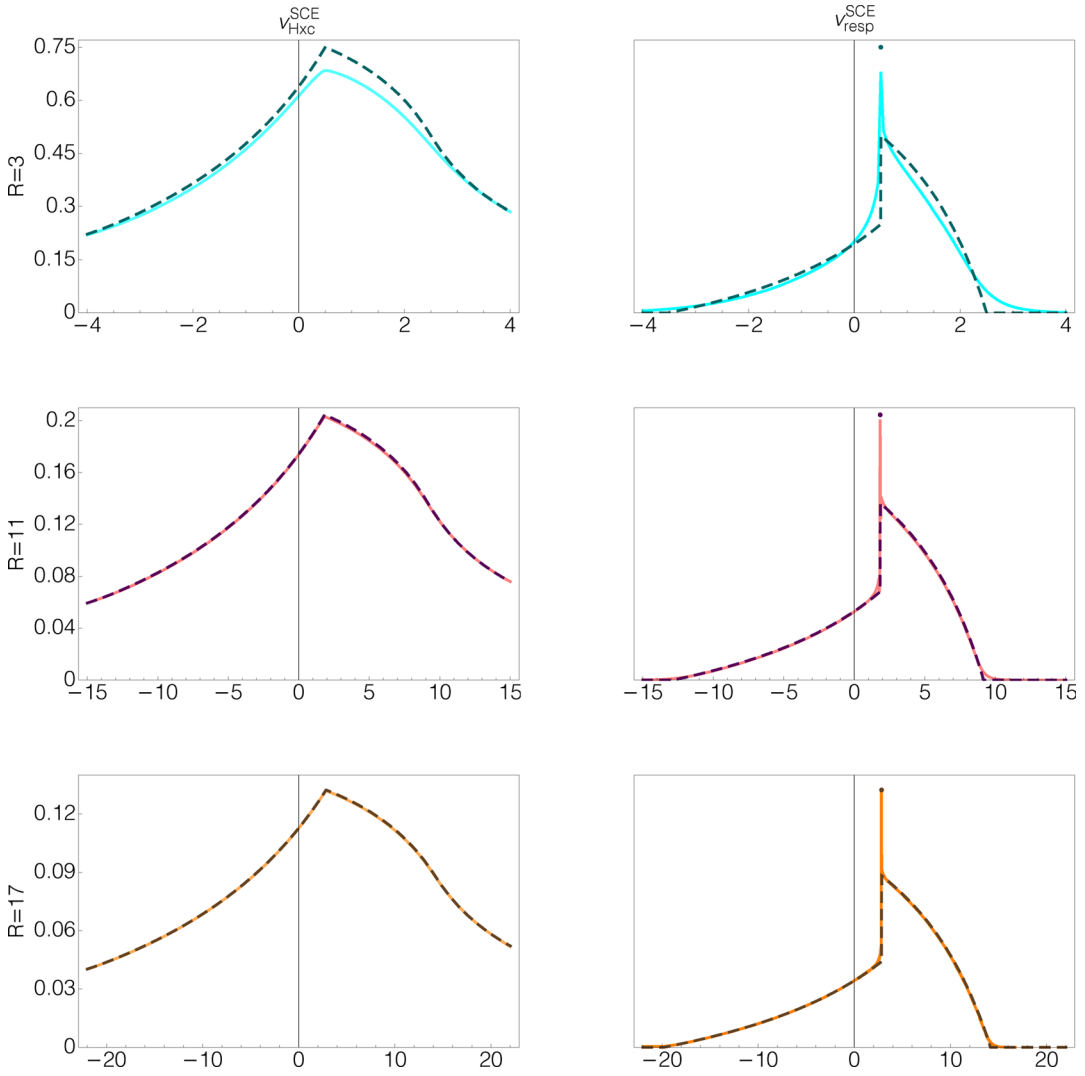

Figure 4. Comparison between the numerical (thick) and the modeled (dashed) v_{Hxc}^{SCE} (right) and the numerical (thick) and the modeled (dashed) v_{resp}^{SCE} at different internuclear distances. Notice that, because within the model the local behavior of the comotion around the divergence is not treated, the response potential $v_{resp}^{SCE}(x)$ shows a pointwise jump in $x = a_R$.

Table 1. Values of the Maximum of v_{Hxc}^{SCE} for the density in eq 61 and the Parameters $a = 2$, $b = 1$ at Different Internuclear Distance, R

	$v_{Hxc}^{SCE}(a_R)$	
R	numerical	modeled
3	0.684	0.75
8	0.278	0.281
11	0.203	0.205
14	0.160	0.161
17	0.132	0.132
20	0.113	0.113

modeled SCE response potential correctly integrates to exactly one as it should, fulfilling a recently derived sum-rule.[55] Moreover, excluding for a moment the point $f_{mod}(a_r) = \infty$ from our model comotion function, we can evaluate the analytical behavior of the step structure of the modeled SCE response potential, $v_{resp,mod}^{SCE}$, that is, the difference from its left and right limits toward a_R, getting

$$\left| \lim_{x \to a_R^+} v_{resp,mod}^{SCE}(x) - \lim_{x \to a_R^-} v_{resp,mod}^{SCE}(x) \right| = \left| \frac{a+b}{2aR} - \frac{a+b}{2bR} \right| = \frac{a^2 - b^2}{2abR} \tag{74}$$

which differs from the exact step height in the model $\left(\frac{a^2}{8} - \frac{b^2}{8}\right)$ by the factor $\frac{a}{2}\frac{b}{2}R$.

CONCLUSIONS AND PERSPECTIVES

We have identified a fundamental difference between two definitions of the XC energy densities and two different decompositions of the XC potential in the fact that, differently than what happens with the global (integrated over all space) expectation values, the conditional amplitude is not stationary for the local Hamiltonian $\hat{h}_\lambda$, preserving first-order terms in the coupling constant, eqs 37−45. This allows us to connect the two different response potentials in the case of a stretched bond (eq

https://dx.doi.org/10.1021/acs.jpca.9b10538
J. Phys. Chem. A 2020, 124, 2473−2482

59). Future works will include the derivation for the case in which the wave function is complex, an analysis of approximate functionals,[28] and the investigation of the relation with response properties of DFT to understand the chemistry.[65]

In addition, we have proposed a working model for the XC and response potential in the strong-coupling limit of DFT for a two-electron stretched dimer, which is very accurate in the dissociation limit. Although restrictied to the 1D case, it could prove useful, for example, to model quantum transport calculations[58] and systems out of equilibrium in hybrid approaches,[66] but also as a starting point to build new approximations that would also include the missing kinetic correlation component.

AUTHOR INFORMATION

Corresponding Authors

Sara Giarrusso − *Department of Theoretical Chemistry and Amsterdam Center for Multiscale Modeling, FEW, Vrije Universiteit, Amsterdam 1081HV, The Netherlands*; Email: s.giarrusso@vu.nl

Paola Gori-Giorgi − *Department of Theoretical Chemistry and Amsterdam Center for Multiscale Modeling, FEW, Vrije Universiteit, Amsterdam 1081HV, The Netherlands*; orcid.org/0000-0002-5952-1172; Email: p.gorigiorgi@vu.nl

Complete contact information is available at: https://pubs.acs.org/10.1021/acs.jpca.9b10538

Notes

The authors declare no competing financial interest.

ACKNOWLEDGMENTS

Financial support was provided by the European Research Council under H2020/ERC Consolidator Grant corr-DFT [Grant No. 648932].

REFERENCES

(1) Almbladh, C. O.; von Barth, U. In *Density functional methods in physics*; Dreizler, R. M., da Providência, J.,, Eds.; Springer, 1985; pp 209−231.

(2) Buijse, M. A.; Baerends, E. J.; Snijders, J. G. Analysis of correlation in terms of exact local potentials: Applications to two-electron systems. *Phys. Rev. A: At., Mol., Opt. Phys.* **1989**, *40*, 4190−4202.

(3) Umrigar, C. J.; Gonze, X. Accurate exchange-correlation potentials and total-energy components for the helium isoelectronic series. *Phys. Rev. A: At., Mol., Opt. Phys.* **1994**, *50*, 3827−3837.

(4) Gritsenko, O.; van Leeuwen, R.; Baerends, E. J. Analysis of electron interaction and atomic shell structure in terms of local potentials. *J. Chem. Phys.* **1994**, *101*, 8955.

(5) Filippi, C.; Gonze, X.; Umrigar, C. J. In *Recent developments and applications in modern DFT*; Seminario, J. M., Ed.; Elsevier: Amsterdam, 1996; pp 295−321.

(6) Baerends, E. J.; Gritsenko, O. V. Effect of molecular dissociation on the exchange-correlation Kohn-Sham potential. *Phys. Rev. A: At., Mol., Opt. Phys.* **1996**, *54*, 1957−1972.

(7) Gritsenko, O. V.; van Leeuwen, R.; Baerends, E. J. Molecular exchange-correlation Kohn-Sham potential and energy density from ab initio first- and second-order density matrices: Examples for XH (X= Li, B, F). *J. Chem. Phys.* **1996**, *104*, 8535.

(8) Baerends, E. J.; Gritsenko, O. V. A Quantum Chemical View of Density Functional Theory. *J. Phys. Chem. A* **1997**, *101*, 5383−5403.

(9) Tempel, D. G.; Martínez, T. J.; Maitra, N. T. Revisiting Molecular Dissociation in Density Functional Theory: A Simple Model. *J. Chem. Theory Comput.* **2009**, *5*, 770−780.

(10) Helbig, N.; Tokatly, I. V.; Rubio, A. Exact Kohn−Sham potential of strongly correlated finite systems. *J. Chem. Phys.* **2009**, *131*, 224105.

(11) Ryabinkin, I. G.; Kohut, S. V.; Staroverov, V. N. Reduction of electronic wave functions to Kohn-Sham effective potentials. *Phys. Rev. Lett.* **2015**, *115*, No. 083001.

(12) Ospadov, E.; Ryabinkin, I. G.; Staroverov, V. N. Improved method for generating exchange-correlation potentials from electronic wave functions. *J. Chem. Phys.* **2017**, *146*, No. 084103.

(13) Cuevas-Saavedra, R.; Ayers, P. W.; Staroverov, V. N. Kohn−Sham exchange-correlation potentials from second-order reduced density matrices. *J. Chem. Phys.* **2015**, *143*, 244116.

(14) Cuevas-Saavedra, R.; Staroverov, V. N. Exact expressions for the Kohn−Sham exchange-correlation potential in terms of wave-function-based quantities. *Mol. Phys.* **2016**, *114*, 1050−1058.

(15) Kohut, S. V.; Polgar, A. M.; Staroverov, V. N. Origin of the step structure of molecular exchange−correlation potentials. *Phys. Chem. Chem. Phys.* **2016**, *18*, 20938−20944.

(16) Hodgson, M. J. P.; Ramsden, J. D.; Godby, R. W. Origin of static and dynamic steps in exact Kohn-Sham potentials. *Phys. Rev. B: Condens. Matter Mater. Phys.* **2016**, *93*, 155146.

(17) Ying, Z.-J.; Brosco, V.; Lopez, G. M.; Varsano, D.; Gori-Giorgi, P.; Lorenzana, J. Anomalous scaling and breakdown of conventional density functional theory methods for the description of Mott phenomena and stretched bonds. *Phys. Rev. B: Condens. Matter Mater. Phys.* **2016**, *94*, No. 075154.

(18) Benítez, A.; Proetto, C. R. Kohn-Sham potential for a strongly correlated finite system with fractional occupancy. *Phys. Rev. A: At., Mol., Opt. Phys.* **2016**, *94*, No. 052506.

(19) Ryabinkin, I. G.; Ospadov, E.; Staroverov, V. N. Exact exchange-correlation potentials of singlet two-electron systems. *J. Chem. Phys.* **2017**, *147*, 164117.

(20) Hodgson, M. J. P.; Kraisler, E.; Schild, A.; Gross, E. K. U. How Interatomic Steps in the Exact Kohn-Sham Potential Relate to Derivative Discontinuities of the Energy. *J. Phys. Chem. Lett.* **2017**, *8*, 5974−5980.

(21) Hunter, G. Conditional Probability Amplitudes in Wave Mechanics. *Int. J. Quantum Chem.* **1975**, *9*, 237−242.

(22) Hunter, G. Ionization Potentials and Conditional Amplitudes. *Int. J. Quantum Chem.* **1975**, *9*, 311−315.

(23) Levy, M.; Perdew, J. P.; Sahni, V. Exact differential equation for the density and ionization energy of a many-particle system. *Phys. Rev. A: At., Mol., Opt. Phys.* **1984**, *30*, 2745−2748.

(24) van Leeuwen, R.; Gritsenko, O.; Baerends, E. J. Step structure in the atomic Kohn-Sham potential. *Z. Phys. D: At., Mol. Clusters* **1995**, *33*, 229−238.

(25) Langreth, D. C.; Perdew, J. P. The exchange-correlation energy of a metallic surface. *Solid State Commun.* **1975**, *17*, 1425−1429.

(26) Perdew, J. P.; Langreth, D. C. Exchange-correlation energy of a metallic surface: Wave-vector analysis. *Phys. Rev. B* **1977**, *15*, 2884−2901.

(27) Gunnarsson, O.; Lundqvist, B. I. Exchange and correlation in atoms, molecules, and solids by the spin-density-functional formalism. *Phys. Rev. B* **1976**, *13*, 4274−4298.

(28) Gritsenko, O.; Mentel, Ł.; Baerends, E. On the errors of local density (LDA) and generalized gradient (GGA) approximations to the Kohn-Sham potential and orbital energies. *J. Chem. Phys.* **2016**, *144*, 204114.

(29) Gori-Giorgi, P.; Gál, T.; Baerends, E. J. Asymptotic behaviour of the electron density and the Kohn−Sham potential in case of a Kohn-Sham HOMO nodal plane. *Mol. Phys.* **2016**, *114*, 1086−1097.

(30) Aschebrock, T.; Armiento, R.; Kümmel, S. Orbital nodal surfaces: Topological challenges for density functionals. *Phys. Rev. B: Condens. Matter Mater. Phys.* **2017**, *95*, 245118.

(31) Gori-Giorgi, P.; Baerends, E. J. Asymptotic nodal planes in the electron density and the potential in the effective equation for the square root of the density. *Eur. Phys. J. B* **2018**, *91*, 160.

(32) Maitra, N. T. Undoing static correlation: Long-range charge transfer in time-dependent density-functional theory. *J. Chem. Phys.* **2005**, *122*, 234104.

(33) Elliott, P.; Fuks, J. I.; Rubio, A.; Maitra, N. T. Universal Dynamical Steps in the Exact Time-Dependent Exchange-Correlation Potential. *Phys. Rev. Lett.* **2012**, *109*, 266404.
(34) Gritsenko, O. V.; Baerends, E. J. Effect of molecular dissociation on the exchange-correlation Kohn-Sham potential. *Phys. Rev. A: At., Mol., Opt. Phys.* **1996**, *54*, 1957−1972.
(35) Levy, M. Universal variational functionals of electron densities, first-order density matrices, and natural spin-orbitals and solution of the v-representability problem. *Proc. Natl. Acad. Sci. U. S. A.* **1979**, *76*, 6062−6065.
(36) Kraisler, E. Asymptotic Behavior of the Exchange-Correlation Energy Density and the Kohn-Sham Potential in Density Functional Theory: Exact Results and Strategy for Approximations. 2019; https://chemrxiv.org/articles/Asymptotic_Behavior_of_the_Exchange-Correlation_Energy_Density_and_the_Kohn-Sham_Potential_in_Density_Functional_Theory_Exact_Results_and_Strategy_for_Approximations/9917189/1.
(37) Kooi, D. P.; Gori-Giorgi, P. Local and global interpolations along the adiabatic connection of DFT: a study at different correlation regimes. *Theor. Chem. Acc.* **2018**, *137*, 166.
(38) Gill, P.; Loos, P.-F. Uniform electron gases. *Theor. Chem. Acc.* **2012**, *131*, 1069.
(39) Loos, P.-F. Exchange functionals based on finite uniform electron gases. *J. Chem. Phys.* **2017**, *146*, 114108.
(40) Freund, D. E.; Huxtable, B. D.; Morgan, J. D. Variational calculations on the helium isoelectronic sequence. *Phys. Rev. A: At., Mol., Opt. Phys.* **1984**, *29*, 980−982.
(41) Teale, A. M.; Coriani, S.; Helgaker, T. The calculation of adiabatic-connection curves from full configuration-interaction densities: Two-electron systems. *J. Chem. Phys.* **2009**, *130*, 104111.
(42) Teale, A. M.; Coriani, S.; Helgaker, T. Accurate calculation and modeling of the adiabatic connection in density functional theory. *J. Chem. Phys.* **2010**, *132*, 164115.
(43) Irons, T. J.; Teale, A. M. The coupling constant averaged exchange−correlation energy density. *Mol. Phys.* **2015**, *114*, 484−497.
(44) Vuckovic, S.; Irons, T. J. P.; Savin, A.; Teale, A. M.; Gori-Giorgi, P. Exchange−correlation functionals via local interpolation along the adiabatic connection. *J. Chem. Theory Comput.* **2016**, *12*, 2598−2610.
(45) Mirtschink, A.; Umrigar, C. J.; Morgan, J. D., III; Gori-Giorgi, P. Energy density functionals from the strong-coupling limit applied to the anions of the He isoelectronic series. *J. Chem. Phys.* **2014**, *140*, 18A532.
(46) Giarrusso, S.; Vuckovic, S.; Gori-Giorgi, P. Response potential in the strong-interaction limit of DFT: Analysis and comparison with the coupling-constant average. *J. Chem. Theory Comput.* **2018**, *14*, 4151−4167.
(47) Becke, A. D. Density-functional exchange-energy approximation with correct asymptotic behavior. *Phys. Rev. A: At., Mol., Opt. Phys.* **1988**, *38*, 3098.
(48) Armiento, R.; Kümmel, S. Orbital Localization, Charge Transfer, and Band Gaps in Semilocal Density-Functional Theory. *Phys. Rev. Lett.* **2013**, *111*, No. 036402.
(49) Seidl, A.; Görling, A.; Vogl, P.; Majewski, J.; Levy, M. Generalized Kohn-Sham schemes and the band-gap problem. *Phys. Rev. B: Condens. Matter Mater. Phys.* **1996**, *53*, 3764.
(50) Mirtschink, A.; Seidl, M.; Gori-Giorgi, P. Energy densities in the strong-interaction limit of density functional theory. *J. Chem. Theory Comput.* **2012**, *8*, 3097−3107.
(51) Wagner, L. O.; Gori-Giorgi, P. Electron avoidance: A nonlocal radius for strong correlation. *Phys. Rev. A: At., Mol., Opt. Phys.* **2014**, *90*, No. 052512.
(52) Bahmann, H.; Zhou, Y.; Ernzerhof, M. The shell model for the exchange-correlation hole in the strong-correlation limit. *J. Chem. Phys.* **2016**, *145*, 124104.
(53) Vuckovic, S.; Gori-Giorgi, P. Simple Fully Nonlocal Density Functionals for Electronic Repulsion Energy. *J. Phys. Chem. Lett.* **2017**, *8*, 2799−2805 PMID: 28581751..
(54) Levy, M.; Perdew, J. P. Hellmann−Feynman, virial, and scaling requisites for the exact universal density functionals. Shape of the correlation potential and diamagnetic susceptibility for atoms. *Phys. Rev. A: At., Mol., Opt. Phys.* **1985**, *32*, 2010−2021.
(55) Giarrusso, S.; Gori-Giorgi, P.; Giesbertz, K. J. Sum-rules of the response potential in the strongly-interacting limit of DFT. *Eur. Phys. J. B* **2018**, *91*, 186.
(56) Lewin, M. Semi-classical limit of the Levy−Lieb functional in Density Functional Theory. *C. R. Math.* **2018**, *356*, 449−455.
(57) Cotar, C.; Friesecke, G.; Klüppelberg, C. Smoothing of transport plans with fixed marginals and rigorous semiclassical limit of the Hohenberg−Kohn functional. *Arch. Ration. Mech. Anal.* **2018**, *228*, 891−922.
(58) Kurth, S.; Stefanucci, G. Dynamical Correction to Linear Kohn-Sham Conductances from Static Density Functional Theory. *Phys. Rev. Lett.* **2013**, *111*, No. 030601.
(59) Seidl, M. Strong-interaction limit of density-functional theory. *Phys. Rev. A: At., Mol., Opt. Phys.* **1999**, *60*, 4387−4395.
(60) Seidl, M.; Gori-Giorgi, P.; Savin, A. Strictly correlated electrons in density-functional theory: A general formulation with applications to spherical densities. *Phys. Rev. A: At., Mol., Opt. Phys.* **2007**, *75*, No. 042511.
(61) Buttazzo, G.; De Pascale, L.; Gori-Giorgi, P. Optimal-transport formulation of electronic density-functional theory. *Phys. Rev. A: At., Mol., Opt. Phys.* **2012**, *85*, No. 062502.
(62) Malet, F.; Gori-Giorgi, P. Strong correlation in Kohn-Sham density functional theory. *Phys. Rev. Lett.* **2012**, *109*, 246402.
(63) Vuckovic, S.; Levy, M.; Gori-Giorgi, P. Augmented potential, energy densities, and virial relations in the weak-and strong-interaction limits of DFT. *J. Chem. Phys.* **2017**, *147*, 214107.
(64) Colombo, M.; De Pascale, L.; Di Marino, S. Multimarginal Optimal Transport Maps for One-dimensional Repulsive Costs. *Canad. J. Math* **2015**, *67*, 350−368.
(65) Geerlings, P.; Boisdenghien, Z.; Proft, F. D.; Fias, S. The $E = E[N,v]$ functional and the linear response function: a conceptual DFT viewpoint. *Theor. Chem. Acc.* **2016**, *135*, 213.
(66) Hopjan, M.; Karlsson, D.; Ydman, S.; Verdozzi, C.; Almbladh, C.-O. Merging Features from Green's Functions and Time Dependent Density Functional Theory: A Route to the Description of Correlated Materials out of Equilibrium? *Phys. Rev. Lett.* **2016**, *116*, 236402.

https://dx.doi.org/10.1021/acs.jpca.9b10538
J. Phys. Chem. A 2020, 124, 2473−2482